

Supporting Information

for

**Enhanced visible light responsive photocatalytic activity of TiO₂-based nanocrystallites:
impact of doping sequence**

Minghui Li, Shujuan Zhang*, Yan Peng, Lu Lv, Bingcai Pan

State Key Laboratory of Pollution Control and Resource Reuse, School of the Environment,
Nanjing University, Nanjing 210023, China

* Corresponding author: Shujuan Zhang

Tel/Fax: 0086-025-89680651

Email address: sjzhang@nju.edu.cn

Table S1. The molecular structure and spectroscopic information of the tested dyes

Dye	Electric property	Molecular structure	Molecular weight	λ_{\max} (nm)	Molar extinction coefficient ($L \cdot mol^{-1} \cdot cm^{-1}$)
AO7	Anionic	azo	350.32	484	15400
MO	Anionic	azo	327.33	463	25500
ARS	Anionic	anthroquinone	342.26	423	3300
BO	Cationic	azo	248.71	442	15300
MG	Cationic	triphenylmethane	364.92	617	43500
RhB	Cationic	triphenylmethane	479.01	552	88400

Figures

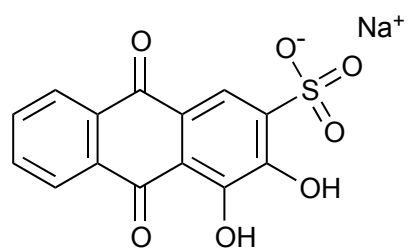
Fig. S1. Molecular structures of the tested dyes.

Fig. S2. XRD patterns of the four doped TiO₂ nanocrystallites.

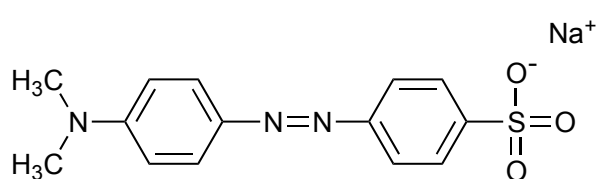
Fig. S3. Particle size distribution of the four doped TiO₂ nanocrystallites.

Fig. S4. Correlation of photocatalytic activity with (a) dopant content, (b) crystallite size, (c) particle size, and (d) specific surface area. Scatter: experimental data, line: linear fitting.

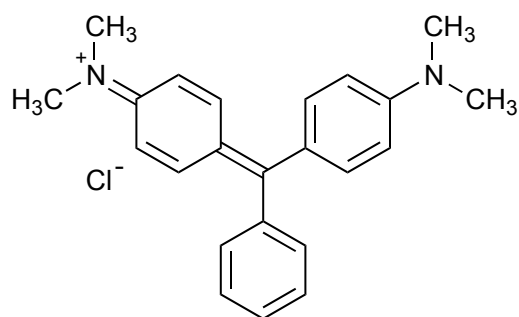
Fig. S5. Zeta potential of the four TiO₂ nanoparticles as a function of solution pH.



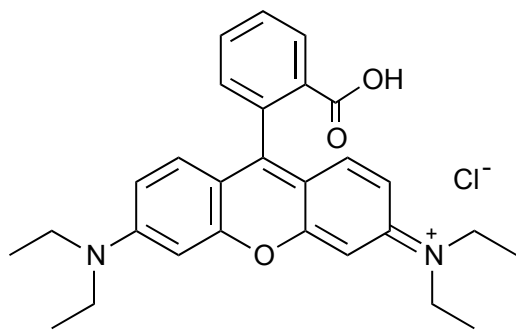
ARS



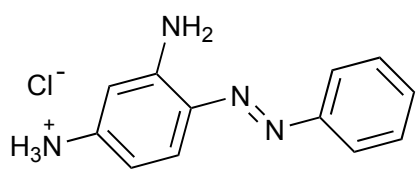
MO



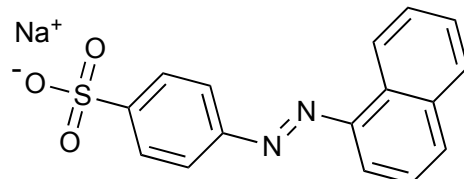
MG



RhB



BO



AO7

Fig. S1

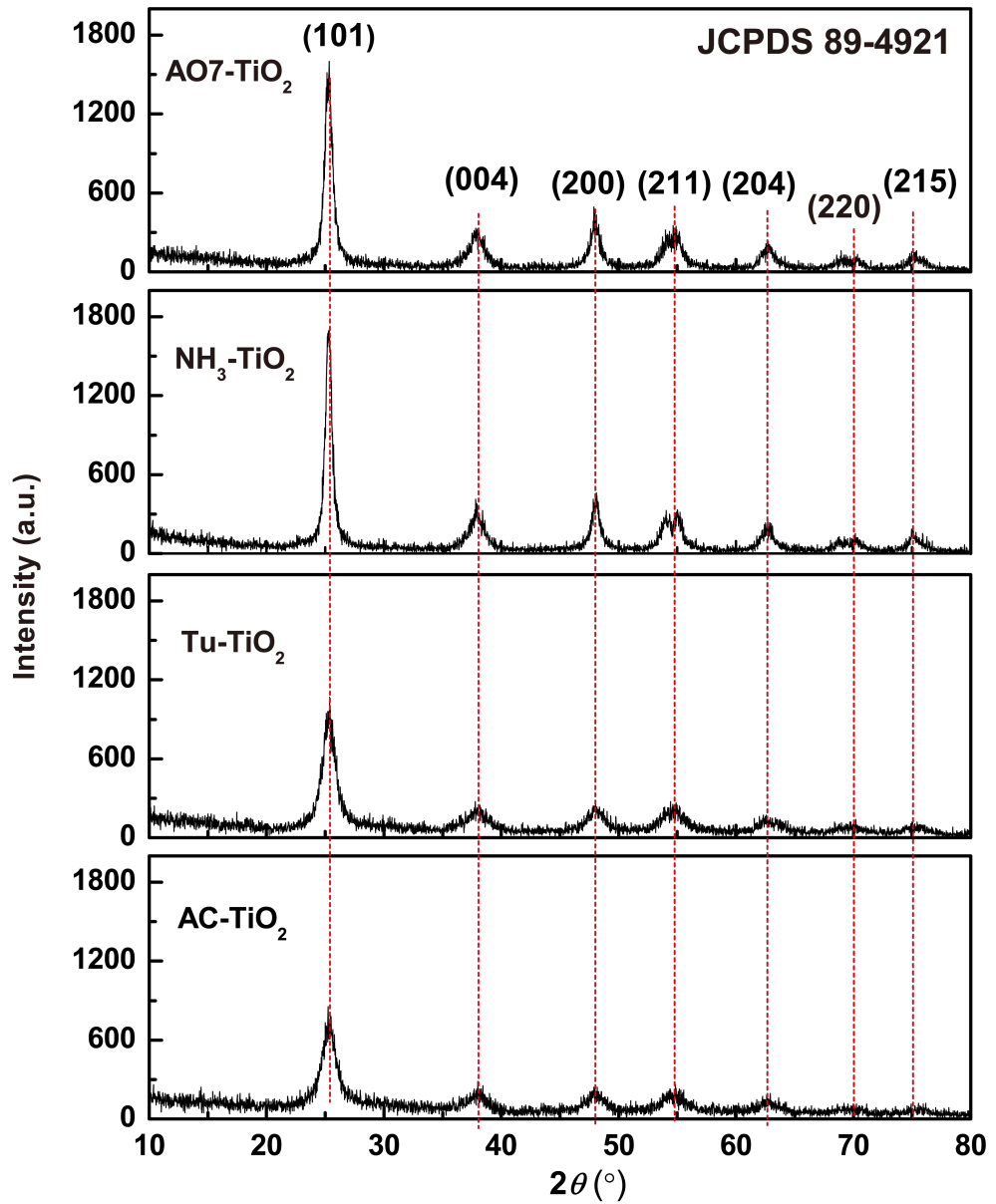


Fig. S2

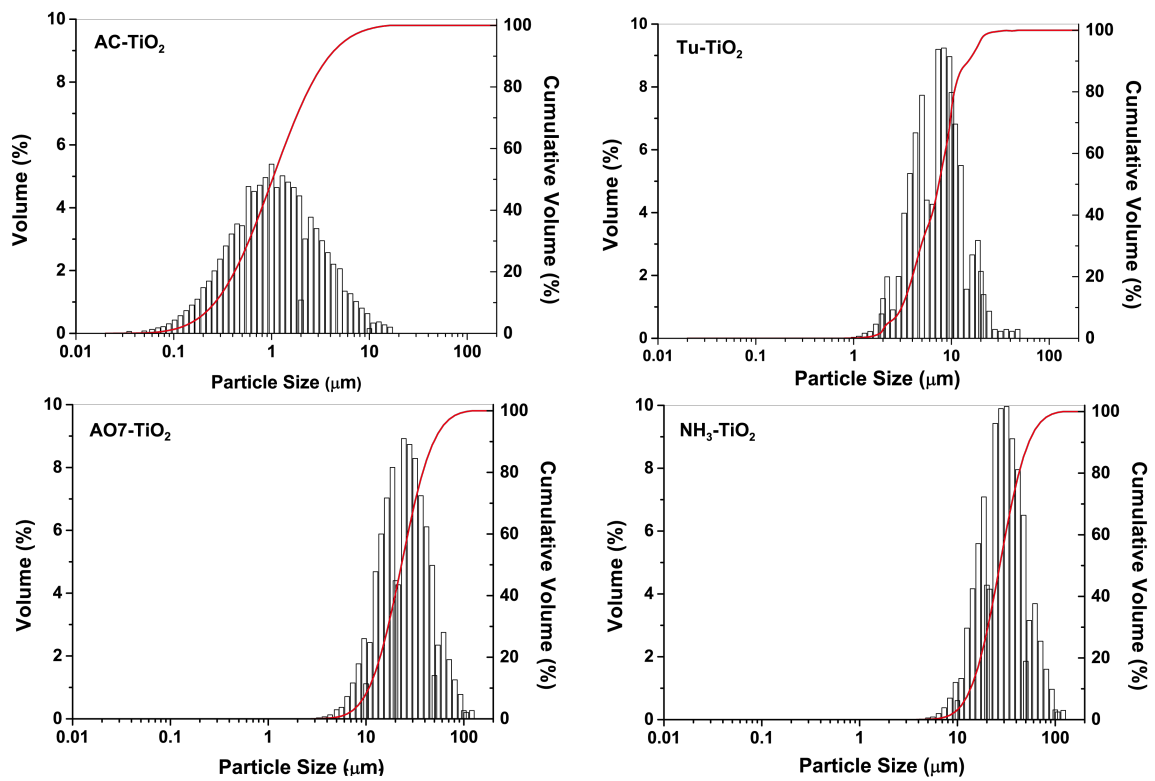


Fig. S3

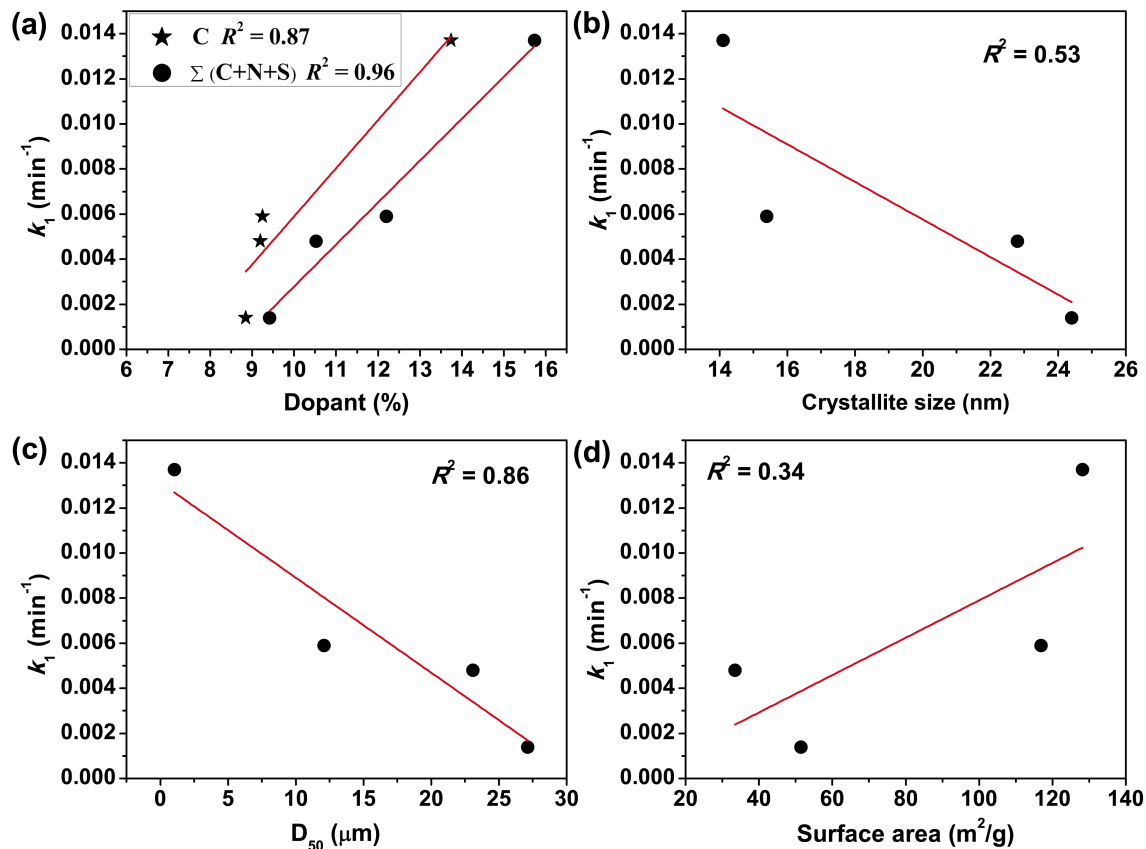


Fig. S4

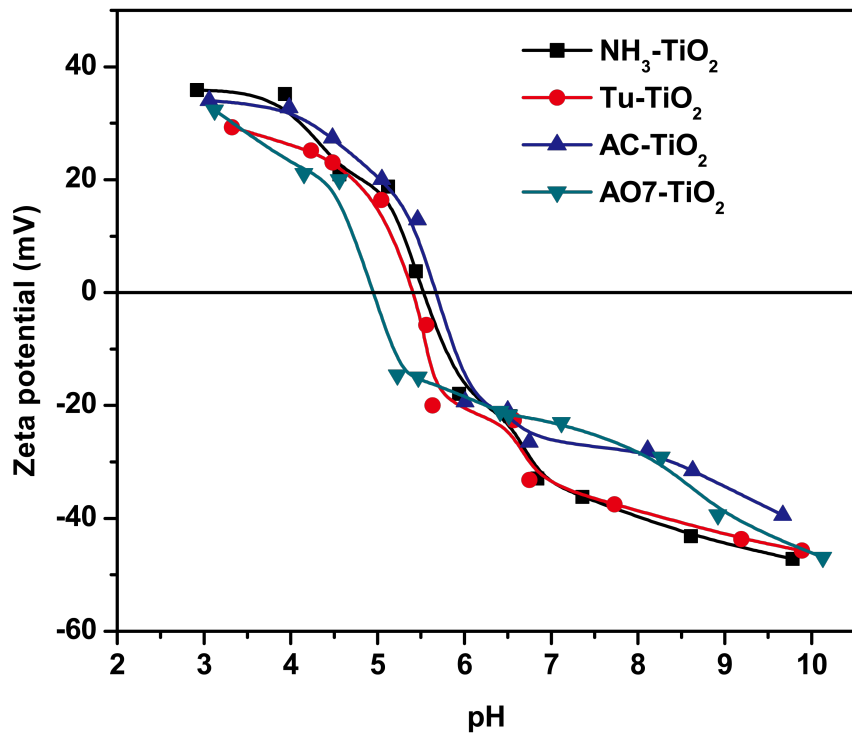


Fig. S5